PETROGRAPHY, MINERAL CHEMISTRY AND METAMORPHISM

5.1. GENERAL

As described in chapter 3, the area mainly comprises Pre-Champaner Gneisses, Champaner Group and Godhra granite. They have been classified as given below;

1. The Pre- Champaner gneiss consists of following rock types;

   A.Pelitic schists

   B.Pelitic gneiss

   C.Micaceous quartzite

   D.Manganiferous and ferruginous quartzite

   E. Granite Gneiss

2. The Champaner Group of rocks, exposed within the study area, mainly consist of crystalline limestone with patches of calcsilicate rocks adjacent to intrusive granite. The associated phyllites, (manganiferous) quartzites and conglomerates, however, do not occur in the study area.

3. Godhra Granite is intrusive granite, which can be classified into two varieties;

   A. Nonfoliated granite

   B Foliated granite.

5.1.1 Pre-Champaner Gneisses: Petrography and Mineral assemblages

A. Pelitic Schists

Three types of pelitic schists can be identified in the study area; i) Sillimanite-muscovite schist, ii). Biotite schist and iii). Kyanite –muscovite schist.

i) Sillimanite-muscovite schist: High alumina metapelite lenses are seen to have associated with the granite gneiss near Vagasthal Hill situated to the east of Chhota Udepur. **(Fig.3.2.4)**. This rock shows fine-grained schistose texture. The schistosity S_1 is defined by parallel alignment of muscovite and fibrolitic sillimanite. At places prismatic sillimanite show chevron type folding (F_2) in microscopic scale. Some of the salient features observed in this rock, are quartz-muscovite symplectite, inclusion of quartz within K-feldspar and cross cutting nature of sillimanite needles (cutting both quartz and muscovite).

ii) Biotite schist

By and large biotite schist comprises of biotite, quartz ±garnet ± sillimanite± cordierite ± plagioclase± K-feldspar. The texture also varies from schistose to gneissose with variable grain size. Biotite schists are exposed mainly in three different localities viz; Wawadi (Sector-II) area Longami area (Sector-V) and Moti Sadli (Sector-VI)) areas . .

Pelitic schists of this region show the following assemblages:

Assemblage: ***A1***) Garnet-biotite-cordierite-K feldspar-quartz-plagioclase.

Assemblage: ***A2***) Sillimanite- cordierite - biotite - K-feldspar- quartz-plagioclase.

Assemblage: ***A3***) Sillimanite- garnet-cordierite - biotite - K-feldspar- quartz- plagioclase.

Assemblage: ***A4***) Garnet- biotite-plagioclase- K-feldspar-quartz.

Assemblage: ***A5***) Garnet- biotite- muscovite –quartz-feldspar

Out of these assemblages minerals of assemblage *A1* and *A3* were analysed by EPMA for geothermometry and geobarometric studies, which are discussed in the ***section 5.4.*** Garnet occurs as porphyroblasts within quartz, K-feldspar, biotite dominated matrix in all garnet bearing assemblages. The S_2 schistosity is defined by preferred orientation of strongly pleochroic dark brown to light brown biotite, elongated strained quartz (showing undulose extinction) and a few muscovite grains.

In Longami- Baroj area (**Sector-V**) equant garnet porphyroblasts are somewhat fractured and contain parallely aligned inclusions of early formed biotite (**Bt_1**), quartz and plagioclase. Outer parts of the garnet crystals are inclusion free. There are a few garnet crystals with straight parallel inclusions that make an angle with the external schistosity (**Fig 5.1**). The S_i in garnet is considered as S_1 and S_e is considered as S_2. Some of the garnet crystals, that are confined within phyllosilicate-rich schistose bands, show elongated habit (lobate/ platong structures (**Fig 5.2.**) and also include some sillimanite crystals in *A3* assemblage.

In Moti Sadli area garnet is recorded in two distinct assemblages viz. *A3* and *A4*. In *A3* assemblage garnet occurs as larger porphyroblastic grains and having a similar textural relationship with biotite and quartz as recorded in Longami. The rocks of this assemblage show well-defined schistosity, where almost all grains except garnet are having preferred dimensional orientation. In Moti Sadli area the rocks show more prominent gneissic banding than Longami area. Generally garnet-bearing assemblage occurs as lenticular patches. In garnet-bearing assemblage, garnet shows internal schistosity defined by quartz, biotite and plagioclase inclusions. Some of the garnet grains are inclusion free whereas some grains contain inclusions in central part with overgrowth of inclusion-free garnet encircling the former. In garnet-free assemblage biotite and sillimanite are seen to have formed fine bands and these two minerals show reaction relationship as seen in thin sections. In garnetiferous biotite schist of Wawadi Hill, garnet occurs as equant porphyroblasts with profuse quartz and biotite inclusions in the central part indicating fast growth rate, whereas the peripheral parts are inclusion free. Here the garnet shows a post-tectonic growth (**Fig. 5.3**).

Cordierite occurs as porphyroblasts as well as within the groundmass. The porphyroblasts are generally xenomorphic and a few are fairly elongated indicating syn- to post-crystallization deformation impact. Some of the grains show characteristic pinitisation, but sector twinning is uncommon. Bearded structure under crossed -nicols is commonly observed. Cordierite in most of the assemblages contains quartz grains and sillimanite needles as inclusions (**Fig. 5.4.**). Rimming of cordierite around corroded garnet crystals also recorded near Longami (**Fig. 5.8**).

In some of the thin sections distinct domain formation are recorded wherein *domain-1* comprising quatzo-feldspathic layers are segregated with coarser fabric and show distinct granoblastic texture in localized scale, whereas in *domain-2* phyllosilicates and garnets are dominant. However, cordierite is seen in both domains. These grains contain considerable amount of biotite, a few quartz grains and sillimanite needles. Quartz-plagioclase-cordierite-dominated bands contain less of biotite and sillimanite.

Sillimanite occurs in *A2* and *A3* assemblages; while in *A2* it occurs as slender inclusion within cordierite, it is seen as larger prismatic grains included within garnet porphyroblasts in *A3* assemblage in Longami-Baroj area (**Fig 5.5**).

Biotite is present in all the assemblages of Longami – Baroj and Moti Sadli areas. They may be classified in two distinct generations. The early-formed biotite (**Bt_1**) are included within garnet porphyroblasts. These are somewhat feebly pleochroic, whereas the matrix biotite (**Bt_2**) is more intensely pleochroic and occasionally contains pleochroic haloes. These are less altered than the included biotite (**Bt_1**). Biotite and quartz often show symplectite texture indicating reaction relation.

Plagioclase is present in most of the assemblages of pelitic schist. In many places they occur in the matrix as xenomorphic grains. At places they are seen to have reacted with the garnet porphyroblasts as seen in assemblages *A1* and *A3*.

K-feldspar, often perthitic, is seen to have developed around partially digested plagioclase in leucocratic micro-bands in association with finer quartz grains.

iii) Kyanite-muscovite schist

This rock type seen is only in Wawadi Kasum area (**Fig 3.2.2.**) It consists of kyanite, muscovite, quartz and K-feldspar. This assemblage is interbanded with garnet –biotite-muscovite schist. Kyanite blades exhibit preferred orientation. As described in *Chapter 3,* tight reclined folds (F_2) have been observed in this area giving rise to distinct mineral lineation ($\mathbf{L_1}$) around $\mathbf{F_2}$ hinges on $\mathbf{S_1}$ surface. Kyanite grains vary in size from *0.3mm* to *1cm* in size. In thin section the grains show 8:1 to 2:1 length/ width ratio. Some of the kyanite grains are also aligned along $\mathbf{S_2}$ (**Fig. 5.6**). Muscovite, quartz and K-feldspar dominate the matrix of the rock. Presence of shadow zones is common on either side of kyanite grains.

B. Pelitic Gneiss

Quartz-muscovite gneiss and quartz- biotite- muscovite gneiss are the dominant metasediments and they occur within this belt as a member of Pre- Champaner Gneiss. This unit occurs around Wawadi and Kasum Villages, around Bordha and north of Sadli areas that fall in the southern part, as well as around Longami and Moti Sadli in the northern and northeastern part of the mapped area. These rocks are characterized by garnet, cordierite and sillimanite in variable proportions. Development of gneissic foliation is the striking feature of these rocks around Wawadi and Kasum Villages. Muscovite constitutes about 25% of the bulk, quartz is about 50%, and rest of the amount is accounted by feldspars.

C. Micaceous quartzite

Micaceous quartzite mainly occur in three localities; (i) in the Goidia Hill as dissected arcuate ridge, (Fig.3.2.1.), (ii) as lenses within pelitic gneiss in Wawadi Hill (Fig.3.2.1) and (iii) in the form of NNW-SSE trending linear ridge near Luni (Fig. 3.2.3.).Variable proportion of muscovite is present in this rock, which in turn has given rise different degree of fissility. Quartz grains show considerable elongation along S_1 planes. In most of the places length and width ratio ranges from 3:1 to 5:1. $\mathbf{S_1}$ is mainly represented by the preferred orientation of muscovite flakes. Some of the muscovite grains show segregation of ferruginous materials along cleavage plains. A few stubby, muscovite grains are seen to have cut across the S_1 schistosity, which probably represent S_2, planes.

D. Manganiferous and ferruginous quartzite

This rock is recorded in the crescent-shaped hills of Goidia, where quartz arenite occurs in alternating bands of magnetite quartzite and mangnaniferous quartzite. The magnetite-bearing quartzite bands vary from 2mm to 15mm in thickness with well-formed octahedral crystals of magnetite. The mangnaniferous quartzites exhibit dark grey to deep brown colour containing both magnetite and pyrolusite and occasionally comprises of pyroxmangite forming thin yellow and reddish bands.

E. Granite Gneiss

This rock belonging to Pre-Champaner Gneisses is intricately deformed as evidenced from different folded structures. The dominance of potash feldspar over plagioclase (about 4 times) is a salient feature of this gneiss. Lenticular patches of biotite schist and gneiss are also recorded at several places within the granite gneiss. It is a well-foliated rock and occasionally exhibits compositional variation. The colour is light pink to grey and is medium grained in nature. It has an average modal composition of microcline (37%), quartz (43%), plagioclase (9%), biotite (7%), and muscovite (1 to 2%), as main phases with some amount of zircon, apatite and magnetite and garnet. Microcline grains generally exhibit well-defined cross-hatched twinning. At few places the gneiss exhibits isoclinal folds, which is also manifested in thin sections, particularly by the preferred orientation of early-formed biotite, which is seen to have been folded. The later formed biotite, cut across the earlier biotite and is parallel to the axial planes of the folds (F_2).

5.1.2. Champaner Group

Champaner Group consist of crystalline dolomitic limestone, nearer to the intrusive granite these have been metamorphosed to calcsilicate rocks like talc- tremolite-actinolite schist, diopside-forsterite/serpentine marble and patches of skarn rocks comprising minerals like wollastonite, andradite, piedmontite, winchite and zoisite. However, impure limestone with variable amount of quartz is the most dominant rock type of the Champner Group present in the study area. The major exposure of this unit is seen to the north of Chhota Udepur, which occur as a large triangular body and also as small linear patch within granite gneiss in the area south of Chhota Udepur Town. However, petrography of this group of rocks has not been dealt in detail.

5.1.3. Godhra Granite

As mentioned in the section 5.1.1 Godhra granite is subdivided into; a) *nonfoliated porphyritic granite* and b) *foliated granite.*

a) Non-Foliated porphyritic granite

Modal analyses of thin sections collected from a porphyritic grey granite indicate 28-32% quartz, 22-30% microcline, 20-36% plagioclase, 6-8% biotite and ~1 % muscovite and other minerals as accessories. Phenocrysts are mainly microcline and often sericitised plagioclase. The accessory minerals are magnetite, apatite and sphene with some zircon. Thin section collected from Bhuwal is essentially composed of quartz, plagioclase, microcline-microperthite and biotite with minor amount of sphene, tourmaline and magnetite. The non-porphyritic pink granite shows hypidiomorphic equigranular texture. Microcline-microperthite occur as larger grains. In porphyritic pink granite microcline occur as phenocrysts, which often show graphic intergrowth with quartz. Quartz occurs as large xenomorphic grains as well as fine grains. Biotite and magnetite form clusters; at places and show diffusion of grain boundary in one another. Biotite grains are strongly pleochroic with a colour change from light brown to deep brown.

Detailed modal analyses with respect to quartz, alkali feldspar and plagioclase for a number of thin sections are shown graphically in Q-A-P diagram (Chapter 6), which was used for classifying the granitic rocks of the area.

b) Foliated Granite

Thin section study of samples indicates that the rock is coarse grained porphyritic and show a crude foliation. Compositionally (both chemical and modal) there is not much of difference between foliated and non-foliated granite. Plagioclase feldspar occurs as larger phenocrysts as well as smaller grains in the groundmass. Often bent and discontinuous deformation twining is noticed in plagioclase. Larger phenocrysts are considerably altered. Inclusions of subhedral biotite grains within sericitised plagioclase are also recorded. Quartz grains are elongated, xenomorphic, often shows marginal granulation. They exhibit strong undulose extinction. Bleb like quartz forms myrmekitic texture within plagioclase.

Microcline generally occurs as phenocrysts. They are strained as indicated by granulation and bending of many grains. Quartz inclusion within microcline phenocrysts in the form of graphic growth is not uncommon. Alteration of biotite into chlorite along cleavages is also recorded. Grain boundary diffusion of biotite into magnetite is also common in many thin sections. Thin section, which have been collected from Nawagan-Longami region, are rich in biotite and exhibit crude gneissic foliation.

5.2. MINERAL CHEMISTRY

Representative minerals have been chemically analysed with a CamecaSX 50 France make model by wavelength dispersive (WDS) spectrometer, sp1, sp2, sp3 electron microprobe with an online sun computer at Geological Survey of India, Faridabad. The instrumental operating conditions for analyses was kept as 20 kV accelerating voltage and 1-micron electron beam size. Polished thin sections of rocks were carbon coated by vacuum evaporating coating technique. A ZAF correction programme has been used for computation of mineral quantitative analysis. The results of chemical analysis of some important minerals involved in the reactions during metamorphism, are shown in **tables 5.1a, 5.1b, 5.2a, 5.2b and 5.2c**. The minerals of assemblage *A1* and *A3* were analysed and are separately shown in the above-mentioned tables.

Garnet: Garnet of both the assemblages *A1* and *A3* are rich in almandine (0.634 to 0.74) with minor pyrope, grossular, andradite and spessertine components. In *A1*, composition of '*spongy part*' of garnet porphyroblasts from spongy central to spongy peripheral range from 0.712 to 0.729 of almandine, 0.156 to 0.138 of pyrope, 0.091 to 0.090 of spessartine, 0.026 to 0.046 of andradite and ~0.011 of grossular. Inclusion free part of the same garnet porphyroblast show composition variation from inner to outer; 0.710 to 0.746 of almandine, 0.163 to 0.105 of pyrope, 0.085 to 0.107 spessertine, 0.029 to 0.011 of andradite and 0.11 to 0.031 of grossular. In *A3* almandine ranges between 0.634 and 0.625 at the central part associated with corresponding pyrope 0.147 and 0.143, spessertine 0.173 and 0.184, andradite 0.033 and 0.068 and grossular 0.014 and 0.02. Rim of the garnet show a composition of almandine 0.654, pyrope 0.107, spessertine 0.194, andradite 0.055 and grossular 0.009. The data show a distinct rise in almandine content in garnet towards rim against a fall in pyrope indicating adjustment during retrograde reaction.

Cordierite: In these assemblages cordierite show cations of Si and Al in the following proportions. Si varies between 4.93 and 4.988 whereas Al varies between 4.022 and 4.089. Cordierite grains do not show compositional zoning, may be because of their margins being commonly replaced by pinites, a possible zoning is obliterated. Systematic compositional variation of cordierite is not recorded. Therefore it is expected that all cordierites formed in similar Pressure –Temperature –Composition (P-T-X) condition. Destabilization of early-formed biotite (Bt_1 Included within garnet) and sillimanite were prompted by the expansion of cordierite phase volume. Between *A1* and *A3*, practically no difference in cordierite composition is noticed and they are chemically more or less homogenous. In *A3*, X_{Fe} (Fe^{+2}/Fe^{+2}+Mg) in Cordierite grains range between 0.386 and 0.42 while in *A1* it varies from 0.393 to 0.408.

Biotite: Compositionally, inclusion- and matrix-biotite(Bt_1 and Bt_2 respectively) do not have much difference with their X_{Mg} ranging between 0.385 and 0.504. In *A1* , included biotite (Bt_1) shows a distinct fall in X_{Fe} and TiO_2 content from core (0.56 and 3.049%) to rim (0.486 and 2.344%) while X_{Fe} and TiO_2 of matrix biotite is 0.486 and 2.46%. In *A3*, included biotite (Bt_1) does not show any change in X_{Fe} (0.56) and TiO_2 (2.867 to 2.831) while matrix biotite shows an appreciable change in X_{Fe} (0.55 to 0.615) and TiO_2 (2.702 to 2.235).

Plagioclase: Plagioclase (X_{An} ranges between 0.392 and 0.4) shows more or less uniform composition in all samples except in one sample of *A3* where plagioclase shows normal zoning (X_{An} Core 0.683 and rim 0.642).

K-feldspar: K- feldspar composition varies from Or 0.841 to 0.912, Ab .086 to 0.157 and An ~ 0.002.

5.3. METAMORPHISM

The Pre-Champaner gneissic complex dominantly consists of gneissic suite of rocks with pelitic schists and quartzite. The gneisses are mainly granite gneiss and quartz-rich pelitic gneiss. The metamorphic history of these rocks could be revealed by studying the mineral assemblages and textures, and thereby possible mineral reactions in these rocks particularly in the pelitic assemblages can be established. To establish Pressure –Temperature – Time **(P-T-t)** path in addition to the mineralogical and textural studies, geothermobarometric studies were also undertaken. The pelitic rocks (schist and gneiss) of Longami area (*Sector-V*; northern fringe of the mapped area, (**Fig.3.2.5**), Moti Sadli area (*Sector-VI;* eastern fringe), Chhota Udepur area (*Sector-V*; central **part,** Fig. **3.2.4**) and Wawadi area (*Sector-II*; southwestern part, **Fig. 3.2.2**) were studied to understand the metamorphic history and the relation between metamorphism and deformation.

5.3.1. Longami area and Moti Sadli area

As mentioned in section **5.1** following metamorphic assemblages are recorded in these localities.

Assemblage: *A1*) Garnet-biotite-cordierite-K feldspar-quartz-plagioclase.

Assemblage: *A2*) Sillimanite- cordierite - biotite - K-feldspar- quartz-plagioclase.

Assemblage: *A3*) Sillimanite- garnet-cordierite - biotite - K-feldspar- quartz- plagioclase.

Assemblage: *A4*) Garnet- biotite-plagioclase- K-feldspar-quartz.

Assemblage: *A5*) Garnet- biotite- muscovite –quartz-feldspar

Schistosity exhibited by biotite, sillimanite (fibrolitic) and lenses of cordierite and quartz is considered as $\mathbf{S_1}$ as it is seen to have been folded during $\mathbf{D_2}$. Garnet is porphyroblastic with spongy central part and inclusion free peripheral part. They include early biotite ($\mathbf{Bt_1}$), quartz and plagioclase in the assemblage *A1* whereas they contain sillimanite, quartz and biotite in assemblage *A2*. Grain size of the internal inclusions in garnets is smaller than their counterparts in the groundmass. Straight and parallely arranged inclusions show an angular relationship with the external schistosity (***Se***). Often quartz-biotite inclusion trails in particular *(S_i)* form a 'S' trail within garnet in *A1* and have an angular relationship with S_e (**Fig.5.1**) Thus garnet porphyroblasts show syn-tectonic growth and they have been enveloped by post-tectonic post-tectonic inclusion free rim.

Elongated garnet grains are recorded with garnetifeous pelitic schist in Longami and also at Wawadi. The elongated garnets are thought to have formed within an active strain field when simultaneously deformation and diffusion to garnet from the matrix took place (Yardly,1981). Similar flattened and elongated garnet has been reported from Grenville Series in southeastern Ontario on regional foliation surfaces along with phyllosilicate. Limited diffusion between garnet on mica-rich foliation surfaces and garnet of quartzofeldspathic layers lead to the contrasting garnet structure and composition. Some of these elongated garnets are highly fractured, amoeboid and suffered stretching leading to platong structure, an evidence of incipient melting. The foliation is very strongly defined by elongated lenses of quartz, K-feldspar and cordierite and preferred lattice orientation of biotite and sillimanite. It has been argued that the assemblage similar to *A1* described, indicate dehydration melting of metapelite (Le Breton & Thomson, 1988). In *A3* and *A4* garnet occurs as porphyroblasts containing inclusion of biotite and sillimanite needles and small equant quartz grains. Modally sillimanite forms 2-3% of the rock and occurs as needles (fibrolite) and prismatic grains (**Fig. 5.4.**). Biotite of second generation (**Bt_2**) occupies about 25% of the rock mass and cut across the early-formed garnet crystals. In assemblage *A3* inclusion biotite (**Bt_1**) and sillimanite needles in cordierite and garnet porphyroblasts indicates a garnet forming reaction.

Textures like inclusion of biotite (**Bt_1**) quartz and plagioclase (**Fig.5.7**) within garnet porphyroblasts in *A1* assemblage can be explained as garnet producing dehydration reaction.

Bt_1 + Qtz +Plag = Gt+ Kfs + H_2O.......Reaction-1 (**R1**) ....(Le Breton & Thomson,1988; Spear & Parrish ,1996)

Or

Bt_1 + Qtz +Plag = Gt+ Kfs + Crd+ H_2O.... *..(R1) .

* where Fe/ Mg of biotite is high...(Henson and Green ; 1971,1972 and 1973)

Sill + Bt_1 +Qtz = Gt + Kfs + H_2O (**R2**) ....(Le Breton & Thomson,1988)

A reaction of muscovite break down in the presence of quartz and plagioclase (**R0**) might have taken place prior to R1 as the initial metamorphic reaction **M_1**, but evidence for R0 could not be put forward as **R1** and **R2** are the metamorphism of **M_1** during peak metamorphic condition.

Mu+ Plg +Qtz = Bt_1+Sill+ Kfs + H_2O.----- **R0**

Muscovite break down reaction in the presence of quartz has taken place in Vagtaldungar (*Sector V*) and Wawadi (*Sector II*) where sillimanite and kyanite formation took place respectively

Mu +Qtz = Sill+ Kfs + H_2O.

Mu +Qtz = Ky+ Kfs + H_2O.---- (Chatterjee and Johannes, 1974)

In assemblage *A3*, inclusion of biotite (**Bt_1**), and sillimanite in cordierite, garnet and K-feldspar indicates a garnet to - cordierite-forming reaction (**R3**). Rimming of cordierite around corroded garnet crystals also indicates a cordierite-forming reaction (**Fig. 5.8**). Elongate habit of the cordierite with oriented sillimanite inclusion (**Fig. 5.4**) supports this reaction and syntectonic growth of cordierite.

4Sill + 2Gt + 5 Qtz → 3 Crd. **R3** (Le Breton and Thomson, 1988)

This is a pressure sensitive reaction with very low negative dT/dP curve.
From the comparison of S_i and S_e relationship in assemblages *A3* and *A1*, it can be concluded that S_1 foliation is synchronous with the digestion of biotite and plagioclase along **S_1** schistosity. The external schistosity (**S_e**), which is corelatable with **S2**, is defined by elongate cordierite, which is having sillimanite inclusions.

The above reaction curve considerably varies in P-T space depending on the Mg/Mg+ Fe in bulk chemical composition. Overgrowth garnets, on which imprints of strong **S_1** schistosity do not persist, are probably developed after **F_1** folding/**D_1** event. The **R3** reaction i.e. cordierite forming reaction appears to have taken place during **M_2** event with a decompression event which led to resorption and disappearance of much of the garnets and formation cordierite.

Following retrograde reactions are likely to have taken place during **F_3** folding event (M_3 metamorphic episode). These reactions are the effect of isobaric cooling.

Crd+ Kfs + H_2O = Mu + Qtz + Bt .... **R4** ...(Le barton and Thomson, op.cit.)

Alteration and digestion of cordierite by muscovite is common in some areas.

Gt + Kfs + H_2O = Bt + Qtz+ Plag **.....R5** (a back reaction of **R1**, not shown in Fig 5.11). Resorption of garnet by late-formed biotite and plagioclase are well recorded in some of the thin sections as corroded garnets are seen to have rimmed by biotite and plagioclase (**Fig**

5.9). Quartz- biotite symplectite is also a evidence of garnet breaking another reaction by isobaric cooling during M_3 **(Fig .5.10)**

The pair cordierite and almandine garnet is restricted to a particular P-T field. Henson and Green (1971, and 1973) have shown that if (MgO+ FeO)/ Al_2O_3 ratio is smaller than 1 in K_2O free system. However, as the rock of this are contains K-feldspar we may consider K_2O as an added phase not involved in the reaction R1.

Resorption of cordierite and garnet by biotite is possible through the following reactions,

Crd + Kfs + H_2O $\rightarrow$ Qtz + Bt_2 +Mus ....**(R4)**

Gt + Kfs + H_2O $\rightarrow$ Bt_2 + Qtz + Plag .... **(R5)**

Study of the texture of the assemblages of Longami and Moti sadli (places where mineral assemblages are similar) can be explained graphically in P-T regime constructing possible reaction curves (**Figure 5.11**) in a multi-component KFMASH system where seven mineral phases and H_2O are present in the system. The mineral phases are sillimanite, cordierite, garnet, biotite, quartz, K-feldspar, plagioclase. As muscovite is absent from all prograde reactions in these areas muscovite invariant situation is interpreted at the center of these reaction bundles.

The possible reaction in Chhota Udepur area (Vagtal Dungar) can be written as

Quartz + Muscovite = Sillimanite + K-feldspar + H_2O ......**R6** .. (Chatterjee and Johannes,1974)

Slope of **R3** is quite gentle and negative in P – T space and formation of garnet and cordierite needs either fall in pressure and / or sufficient increase in temperature. Hydration reaction like **R4** and **R5** act during cooling (**Fig. 5.11**). Resorption of garnet in this assemblage follows reaction **R5** of assemblage *A3*. H_2O required for **R2, R3** and **R5** were presumably supplied by crystallising migmatitic melt. The reactions like **R1**, and **R3** progress towards the right hand side with increase of temperature.

Appearance of cordierite+biotite+alluminosilicate, garnet+biotite+alluminosilicate and cordierite+ garnet+biotite+alluminosilicate in closely space domain indicate overlapping condition for the phase assemblage in iron-rich bulk composition (Spear, 1993).

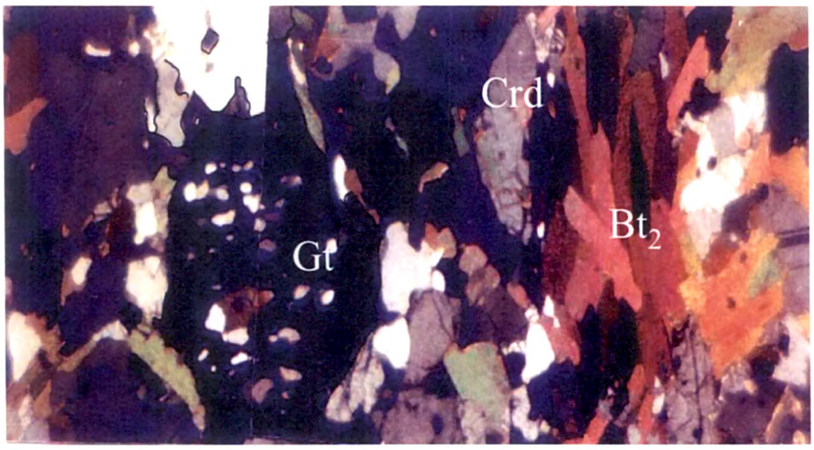

Fig 5.1.
Garnet porphyroblast with straight parallel internal Inclusions. Internal Inclusions make an angle with the external schistosity.

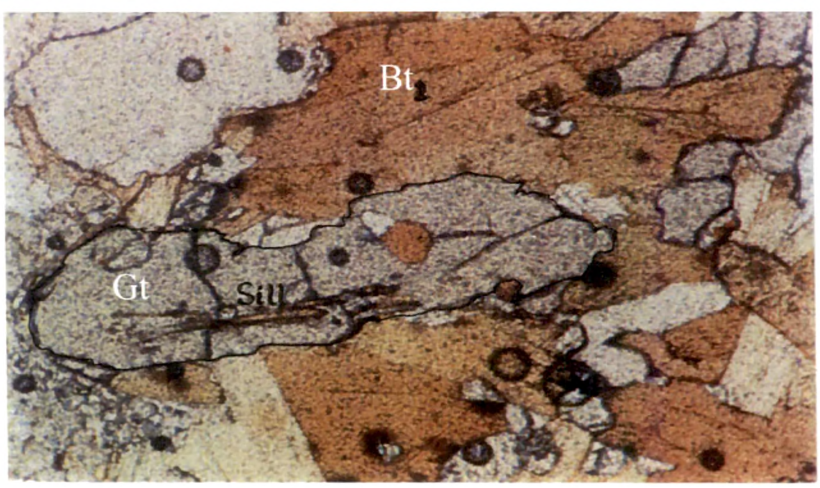

Fig.5.2.
Elongate /Lobate garnet with sillimanite inclusion.

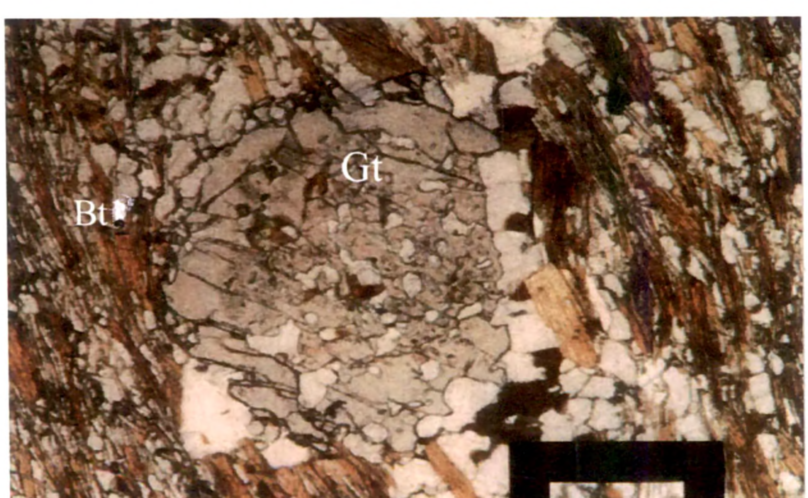

Fig 5.3.
Garnet as equant porphyroblasts with profuse quartz and biotite inclusions in the central part..

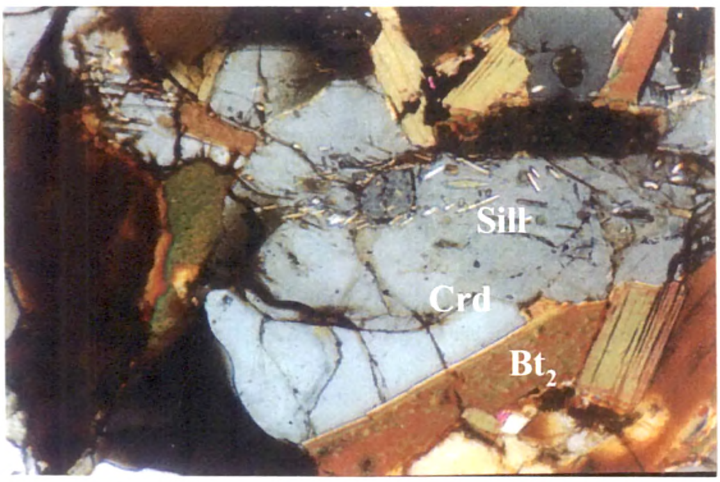

Fig 5.4.
Elongate habit of the cordierite with oriented sillimanite crystals.

Sill=sillimanite,
Crd=cordierite
Bt_2=Biotite

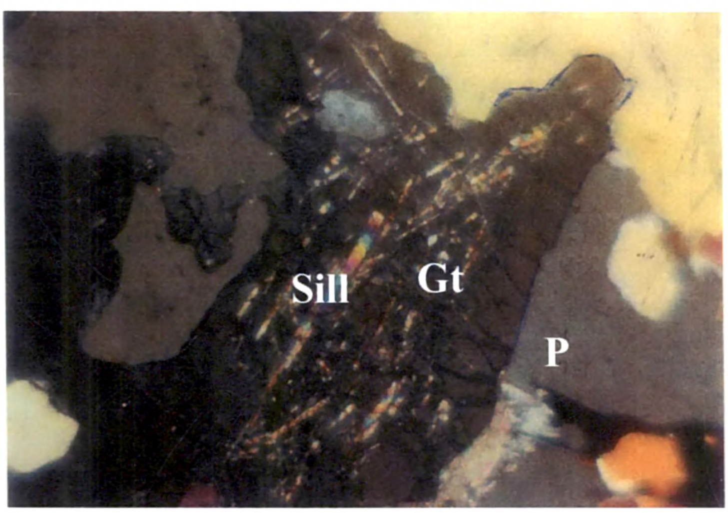

Fig 5.5.
Large prismatic sillimanite grains included within Garnet Porphyroblasts.

Sill=sillimanite,
Gt=Garnet,
P=Plagioclase.

Fig 5.6
Kyanite grains are aligned along S_1 and also along S_2 .

K=Kyanite

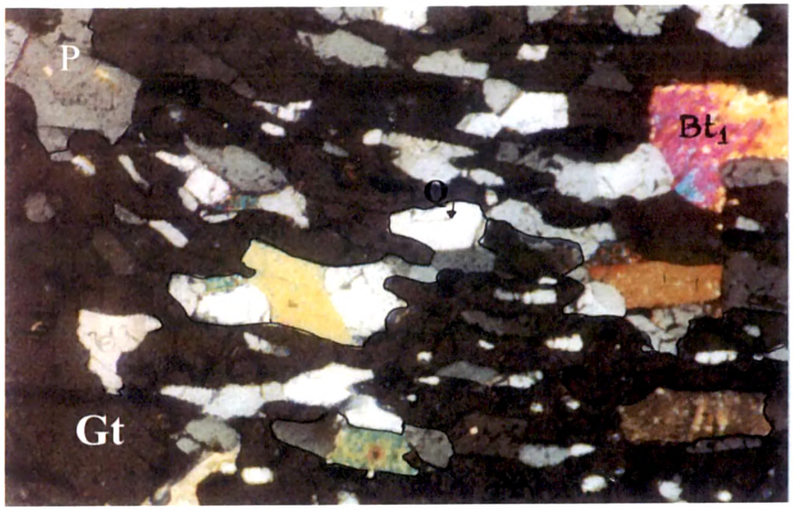

Fig 5.7.Textures like inclusion of biotite (Bt_1), quartz and plagioclase within garnet porphyroblasts indicates garnet producing dehydration reaction.

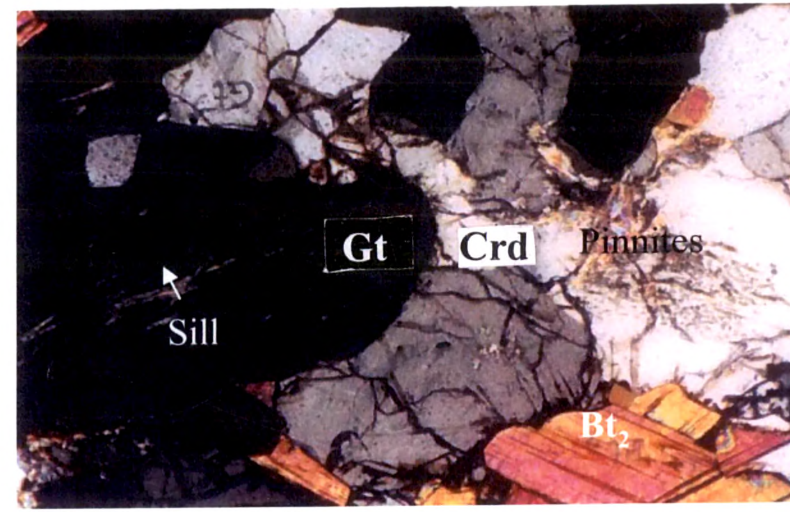

Fig. 5.8 Rimming of cordierite around corroded garnet crystals indicates a cordierite forming reaction.

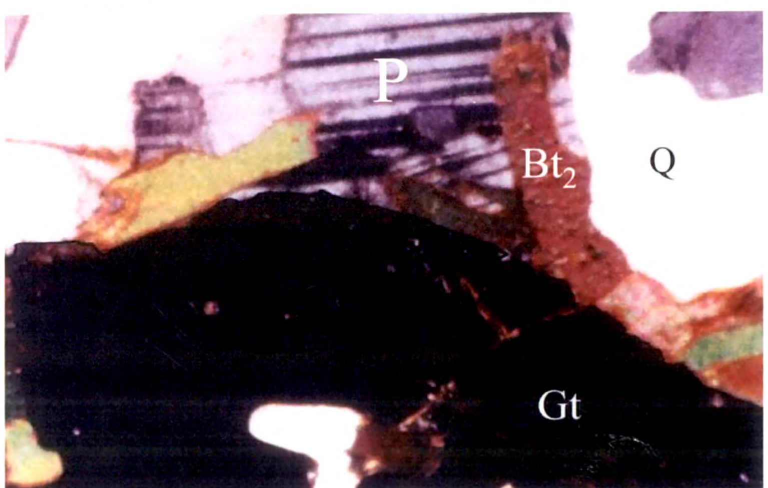

Fig 5.9.Corroded garnet is seen to have rimmed by biotite and plagioclase.

Fig 5.10. Quartz- biotite symplectite is a evidence of garnet breaking reaction by isobaric cooling during M_3

Sp NO	LB 5	LB 5	LB 5	LB 5	LB 5	LB 5	LB 5	LB 5	LB 5	LB 5
Mineral	Garnet	Garnet	Garnet	Garnet	Garnet	Biotite	Biotite	Biotite	Biotite	Biotite
Position	core	Rim	Core	Overgroth	Core	core	core-rim	rim	matrix	matrix
Point	1	18	15	16	17	3	4	5	6	8
SiO2	36.924	36.65	36.965	36.411	37.339	35.196	35.005	35.371	34.99	34.947
Al2O3	21.596	20.92	21.47	21.284	21.69	18.966	18.805	18 826	18.802	19.537
TiO2	0	0	0.045	0.005	0.003	3.049	2.879	2.344	2.46	2.871
Cr2O3	0.2	0.028	0	0	0.107					
Fe2O3	0.934	0.38	0.658	1.623	1.028					
FeO	31.49	32.687	32.128	31.602	31.691	20.549	20.443	18.042	17.263	18.748
MnO	3.974	4.625	3.83	3.887	3.766	0.23	0.05	0.096	0.031	0 123
MgO	3.883	3.582	3.63	3 366	4.084	9.03	8.765	10.252	10.224	8.415
CaO	1.28	1.423	1.326	1.472	1.399					
Na2O	Nil	Nil	Nil	Nil	Nil	0 147	0 163	0 174	0.198	0.171
K2O	Nil	Nil	Nil	Nil	Nil	9.003	8.737	8.68	8.809	8.684
H2O	Nil	Nil	Nil	Nil	Nil	3.955	3.909	3.914	3.88	3.889
Total	100.29	100.295	100.062	99.65	101.11	100.125	98.776	97.773	96.76	97.477
	Structural formula			**X2Y3Si3O12**		**Structural formula**			**X2Y4Z8O20(OH)4**	
Si	2.951	2.985	2.964	2.941	2.956	5.332	5.365	5.414	5 403	5.383
Al iv	0.049	0.015	0.036	0.059	0.044	2.668	2.635	2.585	2.597	2.617
Al vi	1.985	1.99	1.994	1.968	1.98	0.718	0.763	0.81	0.825	0.93
Al total	4.935	4.99	4.95	4.968	4.99					
Ti	0	0	0	0	0	0.347	0.332	0.27	0.286	0.333
Cr	0.013	0.047	0.013	0	0	0	0	0.003	0.004	0.001
Fe 3+	0.052	0.021	0.036	0.091	0.056					
Fe2+	2.11	2.228	2.158	2.143	2.103	2.603	2.62	2.309	2.229	2.415
Mn	0.269	0.319	0.26	0.266	0.253	0.029	0.007	0.012	0.004	0.016
Mg	0.463	0.313	0.435	0.405	0.482	2.039	2.002	2 339	2.353	1.932
Ca	0.11	0.124	0.114	0.127	0.119					
Na						0.043	0.048	0.052	0.059	0.051
K						1.74	1.708	1.695	1.732	1.706
OH						4	4	4	4	4
Tot Oxygen	12	12	12	12	12	20	20	20	20	20
Total cat	8.002	8 039	8.01	7.999	7.993	15.719	15 882	15.489	15.492	15.449
Andradite	0.026	0.011	0 02	0.046	0.029					
Grossular	0.011	0.031	0.019	-0.003	0.011					
Spessar	0.091	0.107	0.088	0.09	0.085					
Pyrope	0.156	0.105	0.146	0.138	0.163					
Almandine	0.712	0.746	0.727	0.729	0.71					

Table 5.1. Mineral chemistry of A1 assemblage of Longami-Baroj area, Pre-Champaner Gneiss

b

Sample no	LB 5	LB 5		LB 5
Mineral	Cordierite	Cordierite		Plagioclase
Position	21	22		11
SiO2	47.775	47.781	SiO2	58.878
Al2O3	32.714	33.199	Al2O3	26.278
TiO2	0	0	TiO2	0
FeO	8.603	9.229	Fe2O3	0 056
MnO	0.307	0.249	MnO	
MgO	7.445	7.534	MgO	
CaO	0.074	0.041	CaO	8.434
Na2O	0.236	0.121	Na2O	6 8
K2O	0.046	0.04	K2O	0 012
P2O5	0.004	0	P2O5	
Cr2O3	0	0		
Total	97.363	98.293	Total	99 764
Si	4.984	4.95		2.599
Al	4.022	4.053		
Ti	0	0.007		
Cr	0			1.391
Fe2+	0.751	0.8		
Mn	0.027	0.022		
Mg	1.158	1.163		0.002
Ca	0.008	0.005		
Na	0.048	0.024		
K	0.006	0.005		0 001
P	0	0	**Or**	0.046
Total	11.017	11.031	**Ab**	.0 017
X Fe	0.393	0.407	**An**	0.07
X Mg	0.61	0.593		

Table 5.1 b Mineral chemistry of A1 assemblage of Longami-Baroj area, Pre-Champaner Gneiss

a

Sp NO	LB 7	LB 7	LB 7	LB 7	LB 7	LB 7	LB 36	LB 36	LB 40	LB 40	LB40
Mineral	Garnet	Garnet	Garnet	Garnet	Garnet	Garnet	Garnet	Garnet	Garnet	Garnet	Garnet
Position	Core	Core-Rim	Core-Rim	Core-Rim	Rim	Core	Rim	Core	Rim	Core	Rim
Point	21	22	23	24	9	run 30	run 46	89	90	71	73
SiO2	36 71	37 02	36 625	37.012	36.965	37 .008	35 79	37 076	36 571	36.873	37 219
Al2O3	21 642	21 286	21 509	21 444	21 613	21 443	21 426	21.095	21 067	21 56	21.713
TiO2	0	0 023	0	0	0	0 005	0	0	0 003	0	0
Cr2O3	0 098	0 004	0	0	0.006	0	0	0	0 048	0 053	0
Fe2O3	1 957	0 435	1 332	0 949	1.901	1 114	2 351	1 5	2 322	0 508	2 28
FeO	27.686	28 39	27 894	28 59	28 797	28 002	26.665	32 058	31.513	33 353	30 687
MnO	7 83	7 769	7 681	7 353	8 459	7 547	8.891	5 401	5 249	4 384	5 226
MgO	3 402	3.368	3 29	3 339	2 82	3 644	2.791	2.532	2 452	3 034	2 378
CaO	1 626	1 623	1 694	1.706	1 577	1.5982	1 56	1 45	1 452	1 654	1 361
Na2O	Nil	Nil	Nil	Nil	Nil	Nil	Nil	Nil	Nil	Nil	Nil
K2O	Nil	Nil	Nil	Nil	Nil	Nil	Nil	Nil	Nil	Nil	Nil
H2O	Nil	Nil	Nil	Nil	Nil	Nil	Nil	Nil	Nil	Nil	Nil
Total	100 958	99 89	100 015	100 5	101 42	100 386	99 621	101 1	100 67	101.17	101 081
		Structural Formula			X2Y3Si3O12						
Si	2 926	2 977	2.944	2 959	2 934	2 958	2 904	2 965	2 935	2 941	2.977
Al iv	0 074	0 023	0 056	0 041	0 049	0.042	0 096	0 035	0 063	0 059	0 023
Al vi	1 959	1 993	1 982	1 98	1 956	1.978	1 954	1 953	1 931	1 967	2 024
Al total	4 959	4 993	4 982	4 98	4 939	4.978	4 954	4 953	4 929	4 967	5.024
Ti	0	0 001	0	0 004	0 003	0	0	0	0	0	0
Cr	0 006	0 003	0	0	0 004			0	0 003	0 004	0 004
Fe 3+	0 109	0 024	0 074	0 053	0 105	0 064	0 142	0.083	0 129	0 088	0
Fe2+	1 854	1 91	1 881	1 915	1.92	1 877	1.82	2.165	2 162	2.143	2 213
Mn	0 592	0 524	0 523	0 498	0 569	0 511	0.611	0.366	0 357	0 296	0.357
Mg	0 404	0 404	0 394	0 404	0.334	0 434	0 338	0 302	0 294	0 361	0 283
Ca	0 139	0 14	0 146	0 146	0 134	0 136	0 135	0 132	0 125	0 141	0 117
OH	Nil	Nil	Nil	Nil	Nil	Nil	Nil	Nil	Nil	Nil	Nil
Tot O	12	12	12	12	12	12	12	12	12	12	12
Tot Cat	8.01	7.99	8	8	8.008	8	8.002	8.001	7.999	8	7.998
Andra	0.055	0.012	0.037	0.03	0.028	0.031		0.042	0.044	0.044	0.027
Grossular	0.005	0.034	0.012	0.02	0.005	0.015	-0.027	0.003	0.014	0.003	0.012
Spessar	0.17	0.176	0.178	0.168	0.194	0.173	0.21	0.123	0.121	0.101	0.12
Pyrope	0.138	0.135	0.134	0.136	0.119	0.147	0.116	0.102	0.115	0.122	0.097
Almandine	0.632	0.641	0.639	0.646	0.654	0.634	0.67	0.73	0.735	0.728	0.744

Sp NO	LB 7	LB7	LB 7	LB7	LB 7
Mineral	Biotite	Biotite	Biotite	Biotite	Biotite
Position	6	7	8	36	6
Point	core	core	rim	matrix	c
SiO2	36 101	35 142	35 775	34 597	36 101
Al2O3	19 758	19 304	19 442	19 251	19 758
TiO2	2 867	2 939	2 831	2 702	2 867
Cr2O3					
Fe2O3					
FeO	19 944	20.059	19 319	18 952	19 944
MnO	0 161	0 143	0 42	0 154	0 161
MgO	8 852	8 581	8 63	8 7	8 852
CaO					
Na2O	0 146	0 197	0 058	0 177	0 146
K2O	8 81	8 878	8 679	8 871	8 81
H2O	4 009	3 931	3 956	3 866	4 009
Total	100 656	99 164	99 244	97 121	100 656
Structural formula	X2Y4Z8O20(OH)4				
Si	5 395	5 396	5 419	5 362	5 395
Al iv	2 605	2 644	2 582	2 638	2 605
Al vi	0 875	0 824	0 888	0 878	0 875
Al total					
Ti	0 322	0 337	0 322	0 315	0 322
Cr	0	0 003	0 003	0 002	0
Fe 3+					
Fe2+	2 493	2 557	2 447	2 456	2 493
Mn	0 02	0 019	0 054	0 02	0 02
Mg	1 972	1 949	1 962	2 01	1 972
Ca					
Na	0 042	0 058	0 017	0 053	0 042
K	1 68	1 707	1 677	1 714	1.68
OH	4	4	4	4	4
Tot O	15 404	15454	15 37	15 448	15 404
X Fe	0.559	0.57	0.555	0.55	0.559
X Mg	0.441	0.43	0.445	0.45	0.441

Fig 5.2a Mineral chemistry of A3 assemblage.Longami -Baroj area.

Sample	LB7	LB 7	LB 7	LB 36	LB 40	LB 9	LB 9
Mineral	PLG	PLG	PLG	PLG	PLG	KFS	KFS
Position	2	3	4	5	6	117	126
SiO2	51.818	50.705	51.749	57.919	57.583	65.178	63.95
Al2O3	31.141	31.601	30.701	26.771	26.983	19.255	18.942
TiO2	0	0	0	0.022	0.066	0	0
Fe2O3	0.048	0.12	0.177	0.048	0.036	0	0.548
MnO	0	0	0			0	0
MgO	0	0.012	0.01	0.017	0.015		
CaO	13.354	14.16	13.611	8.097	8.049	0.036	0.031
Na2O	4.086	3.588	3.986	6.714	6.738	1.611	0.837
K2O	0.047	0.067	0.084	0.247	0.237	13.075	13.441
P2O5							
Total	100.491	100.253	100.319	99..871	99.708	99.165	97.985
Si	2.342	2.303	2.346	2.593	2.583	2.991	2.979
Al	1.658	1.69	1.64	1.413	1.427	1.041	1.04
Ti	0.002	0.004	0.006	0.001	0.001		
Fe3+	nil	nil	nil	0.003	0.002	nil	0.019
Mg++				0.01	0.002		
Ca	0.647	0.689	0.661	0.388	0.387	0.002	0.002
Na	0.358	0.316	0.35	0.583	0.586	0.143	0.076
K	0.003			0.014	0.014	0.765	0.798
P		0.004	0.005				
Total	5.009	5.009	5.009	4.996	5.002	4.943	4.928
Or	0.003	0.004	0.005	0.014	0.014	0.841	0.912
Ab	0.355	0.313	0.345	0.592	0.594	0.157	0.086
An	0.642	0.683	0.65	0.394	0.392	0.002	0.002

PLG=Plagioclase

KFS=K-Feldspar

Table 5.2.b
Mineral chemisrty of A3 assemblage in Longami-Baroj area

Sample no	LB7	LB 7	LB 7	L36	L36	LB 36	LB 40	L9	L9
Mineral	**Cordierite**	**Cordierite**	**Cordierite**	**Cordierite**	**Cordierite**	**Cordierite**	**Cordierite**	**Cordierite**	**Cordierite**
SiO2	48.352	48.419	48.605	48.22	48.226	47.584	48.286	48.56	48.031
Al2O3	33.286	33.282	33.053	33.294	33.741	32.861	33.345	33.367	32.685
TiO2	0	0.03	0.01	0.053	0	0.002	0	0	0
FeO	8.172	8.351	8.074	8.744	8.922	9.35	9.273	9.025	9.282
MnO	0	0		0.177	0	0.538	0.417	0.5	0.532
MgO	7.743	7.841	6.755	7.629	7.624	7.223	7.476	7.254	7.594
CaO	0.002	0.028	0.288	0.025	0.005	0	0.057	0.02	0.017
Na2O	0.135	0.146	0.31	0.154	0.185	0.155	0.226	0.175	0.148
K2O	0.027	0.018	0.164	0.001	0.011	0.002	0	0.057	0
P2O5	0	0	0.155	0	0.027	0	0.025	0	0.009
Cr2O3	0	0	0.079	0	0.039	0	0	0.018	0
Total	98.55	98.23	97.107	98.345	98.989	97.784	99.125	99.111	98.309
Si	4.995	4.985	4.962	4.955	4.954	4.965	4.963	4.988	4.981
Al	4.061	4.024	3.998	3.995	4.085	4.041	4.039	4.039	3.998
Ti	0	0	0.007	0	0	0	0	0	0
Cr				0	0.003				
Fe2+	0.735	0.744	0.81	0.751	0.766	0.816	0.797	0.775	0.805
Mn	0.034	0.027	0.23	0.025	0	0.048	0.036		
Mg	1.17	1.173	1.17	1.19	1.167	1.123	1.145	1.111	1.174
Ca	0.004	0.008	0.005	0.003	0	0	0.006	0.002	0.002
Na	0.022	0.048	0.024	0.04	0.037	0.031	0.045	0.035	0.03
K	0.002	0.006	0.005	0.001	0.001	0	0	0.007	0
P	0.007	0.009	0.001	0	0.002	0.001	0.002	0	0
Total	11.03	11.024	11.03	11.035	11.018	11.03	11.03	11.036	11.013
X Fe	0.385	0.388	0.41	0.386	0.396	0.421	0.41	0.64	0.406
X Mg	0.615	0.612	0.59	0.614	0.604	0.579	0.59	0.36	0.606

Table 5.2.c
Mineral chemisrty of A3 assemblage in Longami-Baroj area

5.4. DEFORMATION AND METAMORPHISM

Correlation between deformation and metamorphism is possible for early folding and metamorphic events (**F_1 - M_1** and **F2 - M_2**). The relict deformation structures preserved in garnet as well as within the garnet bearing quartzo-feldspathic bands in Longami and Moti sadli area clearly indicates that these are result of **M_1** (early prograde metamorphism),which is related to **F_1** folding event. Elongated garnet was synkinametically grown along **S_1** subsequently it was affected by **D_2 (Plate 4.2.C)**)where **S_2** makes a low angle. Similarly the kyanite bearing muscovite schist and elongated porphyroblasts bearing garnetiferous biotite schist indicate **M_1** was synkynametic with **F_1** folding event. Overgrowth garnet, which has been escaped **F_1** folding event, seem to have grown postkinematically as **M_1** continued after the early deformation. Resorption of garnet and sillimanite by formation of cordierite during **M_2** (decompression reaction, **R3**) is common. Formation of cordierite was synkynametic with **S_2** formation during **D_2**. Biotite and plagioclase and formation from garnet and muscovite and late biotite at the expense of cordierite were possible for the hydration reactions **R4** and **R5** during **M_3**.

5.5. GEOTHERMOBAROMETRY

It is well known that the garnet –biotite Fe-Mg exchange geothermometer is most widely accepted and used thermometer for estimating T equilibrium of medium grade metapelites. Calibrations were pioneered by Ferry and Spear (1978) who considered ideal solutions of these pairs. A revised geothermometric calibration has been done by Holdaway et el.(1997) that takes care of many of the drawbacks of earlier calibration including non-ideality in garnet and biotite. To have consistent data geothermometric calibrations by Ferry and Spear(1978) and Holdaway et al (1997) have been adopted in this work.

Pressure – Temperature close to peak metamorphic condition can only be retrieved from the core compositions of the porphyroblastic phases stabilized at that condition. Extensive resetting of garnet biotite composition hinders retrieving peak temperatures in these assemblages. Garnet- biotite exchange thermometers for garnet core and matrix biotite registers temperatures as high as 781°C (Ferry and Spear,1978) and 768°C (Holdaway et al,1997) which is shown in **Table 5.3**. Minimum temperature recorded through this method is 616°C (Ferry and Spear, 1978) and 605°C (Holdaway et al, 1997).

Pressure cannot be retrieved using compositions of garnet, plagioclase, aluminosilicate and quartz (GAPQ) barometer in these assemblages due to the extremely low grossular content in garnet. Pressure for cordierite formation for both *A1* and *A3* assemblages are derived from garnet, cordierite, alluminosilicate and quartz barometer (Bhattacharya, 1986) at estimated mean of 732°C, ranging between 3.8 to 4.1 Kb (**Table -5.4.**). The peak metamorphic condition was during $\mathbf{M_1}$ when garnet formed at the expense of biotite and aluminosilicate.

No P–T estimation is possible in greenschist facies rocks of Champaner Group, due to lack of proper assemblages but non-appearance of chloritoid in these rocks helps in assuming a temperature c.a. 500°C at 3 Kb when $\mathbf{M_3}$ took place.

Mineralogical geothermobarometers has several limitations, though these can be applied purposefully for determination of thermobarometric evolution. Often, only discrete P–T points on the total path of P–T trajectory of evolution of metamorphic complexes can be estimated. Keeping this in mind, the recorded P–T data in Tables **5.2** & **5.3** are synthesized. The T_{max} values are obtained from core compositions of the porphyroblastic phases.

The recorded T_{max} in the study area is ~780°C and this must be close to peak conditions since extensive melting in biotite bearing parent material did not take place. However, production of quartzo-feldspathic layers in the study area hints some degree of melting. Formation of cordierite from garnet is pressure sensitive and started below 4 Kb in all the assemblages. Formation of garnet and cordierite in this part of Pre-Champaner Gneisses can be achieved through simple change of temperature around pressure of 4Kb. It is observed that other dehydration reaction **R1** also shifts from left-hand side to the right-hand side, indicate that P–T conditions during progressive metamorphism in response to heating within sillimanite field. Gradual decrease of kyanite schist pockets from the western part to eastern part and final disappearance kyanite and being substituted by sillimanite schist is indicative of unidirectional change of P-T condition at the regional scale. However, this can only occur in response to heating at pressure above the triple point i.e., ~ 4 Kb. Retrogressive events were marked by an isobaric entry to green schist facies by cooling. Thus in this area the metamorphic reaction follows a clockwise path, i.e. high temperature progressive metamorphism at isobaric condition- first, followed by decompression at constant temperature and then retrogression with cooling at almost constant pressure (**Fig 5.11**). In this study area thus a clockwise P-T-t path is observed, whereas an anticlockwise path was observed by Guha and Bhattacharya (1995) in Sandmata Complex of BGC. This aspect is further discussed in chapter 7.

Table 5.3. Estimation of temperature from *A1* and *A3* pelitic assemblages of Pre-Champaner Gneisses.

Assemblage	Sample No	Garnet-Biotite Pair (Analysis point and position)	Ln Kd	Temperature in (°C)			
				Ferry & Spear,'78		Holdaway et al, '97	
A1	LB 5	(core- matrix)	-1.361	726	742 *	717	729 **
	LB 5	(core-matrix)	-1.295	757		742	
A3	LB 7	(core-matrix)	-1.249	781	700 $	768	687 $$
	LB 7	(core- matrix)	-1.323	745		729	
	LB 7	(rim-rim)	-1.356	728		717	
	LB 7	(rim-rim)	-1.478	675		661	
	LB 36	(core-matrix)	-1.570	638		632	
	L36	(core-matrix)	-1.497	668		652	
	L40	(core-matrix)	-1.313	749		735	
	L40	(rim – rim)	-1.58	616		605	

* = Average temperature deduced from *A1* assemblage using Ferry & spear thermometer.

$ = Average temperature deduced from *A3* assemblage using Ferry & spear thermometer.

** = Average temperature deduced from *A1* assemblage using Holdaway et al. thermometer.

$$ = Average temperature deduced from *A3* assemblage using Holdaway et al. thermometer.

Table 5.4: Estimation of Pressure from A1 and A3 Assemblages of Pre-Champaner Gneisses.

Assemblage	Sample no	Garnet-Cordierite Pair (analysis point and position	Ln Kd	Pressure (Kb)	Average pressure for individual assemblage (Kb)
A1	LB5	15 & 21(core- crd inclusion core).	0.647	4.08	3.95
	LB5	1 & 22 (core- matrix)	0.593	3.88	
	LB5	15 & 22(core-matrix)	0.606	3.90	
A3	LB7	21 & 109 (core-matrix)	0.581	3.86	3.87
	LB7	22 & 112 (core-rim)	0.566	3.82	
	LB36	89 & 88 (core- crd inclusion core)	0.571	3.84	
	LB40	71 & 81(core- matrix)	0.610	3.94	
	LB40	71 & 75 (core - matrix)	0.6	3.92	
	LB7	9 & 41 (rim-rim)	0.548	3.81	

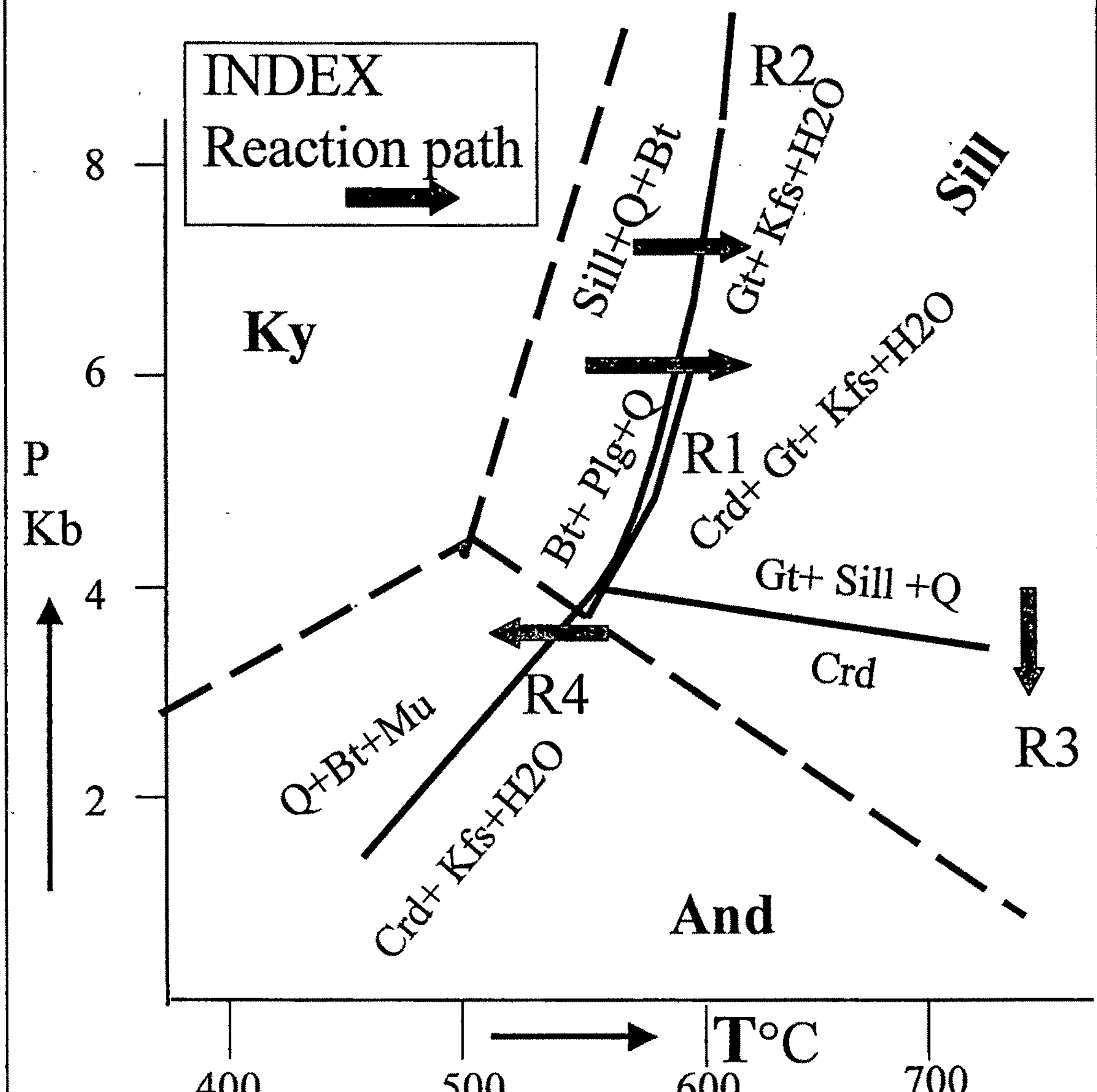

Fig.5.11. Semiquantitative P-T-t path derived from the pelitic assemblages of Pre-Champaner Gneisses. Ky=Kyanite field, Sill=Sillimanite field, And=Andalusite field